Anchors in Theory and Practice, Widmann (ed.) © 1995 Balkema, Rotterdam. ISBN 90 5410 577 1

Passive resistance of strip anchors

Passiver Widerstand von Plattenankern

P. Regenass & A. H. Soubra
École Nationale Supérieure des Arts et Industries de Strasbourg, France

ABSTRACT: This paper describes an upper bound method in limit analysis for calculating the ultimate load of plate anchors. The present analysis considers the general case of a frictional and cohesive soil with an eventual surcharge loading on the ground surface. Three translational failure mechanisms are considered for the calculation schemes. The numerical results obtained from the different mechanisms are presented in the form of non dimensional coefficients. They show that the increase of the embedment depth significantly increases the ultimate load. The same phenomena is also valid for the anchor inclination. Finally, the effect of the anchor inclination on the critical slip surface is presented. It shows that the slip surface tends to a planar surface when the anchor inclination decreases.

ZUSAMMENFASSUNG: Diese Studie stellt ein Berechnungsverfahren vor, das es erlauben soll, die Belastungsgrenze von Plattenankern rechnerisch zu bestimmen. Es handelt sich dabei um einen kohärenten, schwimmenden Boden, bei dem eine zusätzliche Belastung an der Bodenoberfläche berücksichtigt werden kann. Drei Übertragungsmechanismen werden dabei in Betracht gezogen. Die an Hand dieser Mechanismen erzielten Ergebnisse werden in Form adimensionaler Koeffiziente ausgedrückt. Wir zeigen dabei, daß die Belastungsgrenze wesentlich mit der Verankerungstiefe ansteigt. Ähnlich verhält es sich mit der Neigung der Verankerung. Der Einfluß der Neigung der Verankerung wird auf der äußersten Gleitlinie dargestellt. Dabei hat sich herausgestellt, daß sich diese Gleitlinie bei einer geringen Neigung der Verankerung einer Geraden nähert.

1 INTRODUCTION

The problem of the passive resistance of anchors has been widely studied in literature: Smith (1962), Smith & Stalcup (1966), Ovesen & Stroman (1972), Neely et al (1973), Das & Seely (1975), Rowe & Davis (1982), Dickin & Leung (1983) and Murray & Geddes (1989). In this paper, we focus our study on the determination of the ultimate load of strip anchors.

In fact, this problem belongs to the stability problems in geotechnical engineering and it has been modelled by either the limit equilibrium methods, the slip line methods or the limit analysis methods.

While the limit equilibrium methods are simple, the slip line methods are more complicated since they require the establishment of a stress field in the plastically deformed region. Notice however that these methods do not allow to know if the solution obtained is an upper or a lower bound one with respect to the exact solution for an associated flow rule material.

The limit analysis method is based on the limit theorems of Drucker et al (1952) and it is employed to obtain upper and lower bounds of the collapse load using the upper and lower bound methods.

It is to be noted that the lower bound method in limit analysis has not been widely used in geotechnical engineering since it is so complex for obtaining the statically admissible stress field in the soil mass. However, due to the facility of establishment of kinematically admissible mechanisms, the upper bound method has been used by Chen (1975) who presented the solutions for many stability problems in geotechnical engineering by using different failure mechanisms.

In this paper, we present an upper bound

method in limit analysis to calculate the ultimate load of strip anchors. Three failure mechanisms are considered for the calculation schemes : These mechanisms are of the translational type as it will be shown later in the following sections. They are a generalisation of three failure mechanisms considered by Chen (1975) in the passive earth pressure problem and reviewed by Murray & Geddes (1989) for the calculation of the ultimate failure load of strip anchors. Notice that Murray & Geddes (1989) have considered the case of a cohesionless soil.

The present analysis will consider the general case of a frictional and cohesive (c, ϕ) soil. The ultimate failure load due to soil weight, soil cohesion and surcharge loading on the ground surface is given in the form of non dimensional anchor force coefficients M_γ, M_c and M_q.

2 HYPOTHESES

For the problem of computation of the ultimate failure loads of strip anchors, the following assumptions will be adopted here:

- As shown in figure (1), the anchor plate is characterised by its breadth h, its embedment depth H and its inclination ψ.

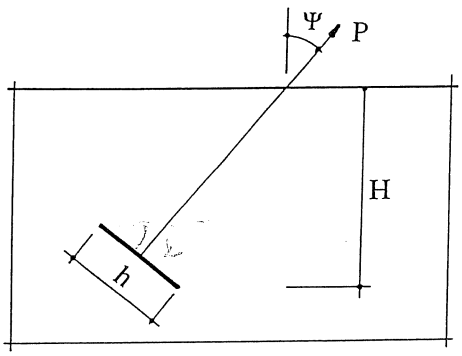

Figure 1 : Strip Anchor, Notations
Abbildung 1 : Plattenanker, Bezeichnungen

- The soil is assumed to be an associated flow rule Coulomb material obeying Hill's maximal work principle. It is characterised by its angle of internal friction ϕ and its cohesion c.
- The angle of friction δ at the soil-structure interface is assumed to be constant. This hypothesis is in conformity with the kinematics assumed in this paper as it will be shown later in this paper.
- An eventual uniform surcharge loading can act at the soil surface which is assumed to be horizontal.
- The assumption of a sliding by friction is adopted at the soil-structure interface. Hence, the velocity at this interface is tangent to the anchor plate.

3 THEORETICAL ANALYSIS

According to the upper bound theorem in limit analysis, for a kinematically admissible velocity field, an upper bound of the exact collapse load can be obtained by equating the power dissipated internally to the power expended by the external loads.

A kinematically admissible velocity field is one that satisfies the flow rule, the velocity boundary conditions and compatibility. During plastic flow, power is assumed to be dissipated by plastic yielding of the soil mass, as well as by sliding along velocity discontinuities where jumps in the normal and tangential velocities may occur.

Note that the velocity field at collapse is often modelled by a mechanism of rigid blocks that move with constant velocities. Since no general plastic deformation of the soil mass is permitted to occur, the power is dissipated solely at the interfaces between adjacent blocks, which constitute velocity discontinuities. This kind of velocity field will be used herein. Finally, note that in the case of the ultimate load of strip anchors, the upper-bound theorem gives an unsafe estimate of the failure load.

In this paper, three failure translational mechanisms are considered for the calculation of the ultimate failure load. These mechanisms will be refereed to as the M_1, M_2 and M_3 mechanisms. They are described in the following sections.

3.1 Mechanism M_1

As shown in figure (2), this mechanism is composed of a single rigid bloc moving with velocity V_1. The anchor plate moves with the velocity V_0 and V_{01} represents the relative velocity at the soil-structure interface.

This mechanism is kinematically admissible since the velocity along the velocity

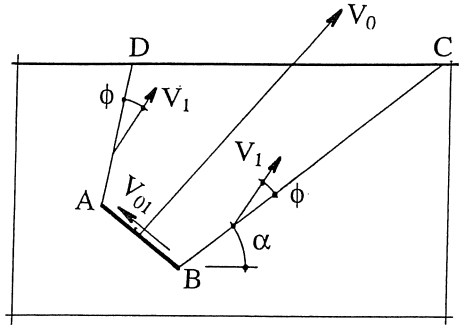

Figure 2 : Mechanism M_1
Abbildung 2 : Mechanismus M_1

discontinuities AD and BC makes an angle ϕ with these surfaces : It is characterised by a single parameter α.

3.2 Mechanism M_2

As shown in figure (3), this mechanism is composed of two rigid blocs ABC and ACDE moving respectively with velocities V_1 and V_2. V_{12} represents the relative velocity at the discontinuity surface AC while V_{01} is as defined above.

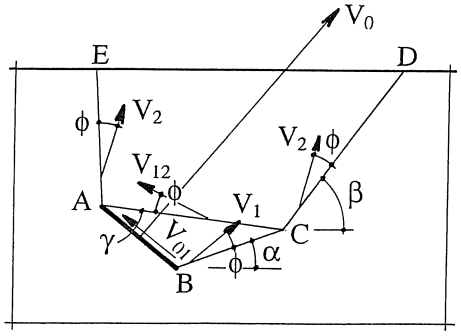

Figure 3 : Mechanism M_2
Abbildung 3 : Mechanismus M_2

This mechanism is kinematically admissible since it verifies all the kinematical constraints mentioned above. This collapse mechanism depends on three angular parameters α, β and γ. These angular parameters describe completely the failure surface.

3.3 Mechanism M_3

As shown in figure (4), this mechanism is composed of a radial shear zone AEF sandwiched between two rigid blocs ABE and AFCD.

The radial shear zone is limited by a log spiral slip surface EF. The log spiral slip surface is tangent to lines BE and FC respectively at points E and F.

The rigid blocs ABE and AFCD move respectively with the velocities V_1 and V_2.

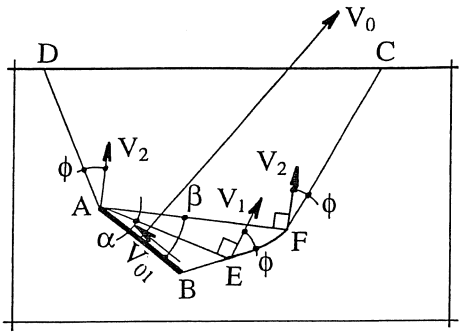

Figure 4 : Mechanism M_3
Abbildung 4 : Mechanismus M_3

It is to be noted here that due to the fact that the log spiral is tangent to lines BE and FC, there is no velocity discontinuities along lines AE and AF. It was shown by Chen (1975) that the velocity distribution along the log spiral slip surface is given by:

$$V(\theta) = V_1 . \exp((\theta - \alpha)\tan\phi) \qquad (1)$$

This mechanism is kinematically admissible and it is completely defined by two angular parameters α and β. It will be named the log sandwich mechanism as made by Chen (1975) for the earth pressure problem.

3.4 Work equation

For each of the three failure mechanisms, one can write the work equation by equating the rate of external work done by the external forces to the rate of internal energy dissipation along the plastically deformed surfaces.

Finally, one can obtain the critical failure load after extremization of the 'potential' failure load as it will be shown in the following sections.

The incremental external work due to an external force is the external force multiplied by the corresponding incremental displacement or velocity.

The external forces contributing in the incremental external work consist of the load anchor, the weight of the soil mass and the surcharge q at the ground surface.

The incremental external work due to self weight in a region is the vertical component of the velocity in that region multiplied by the weight of the region. The incremental external work for the different external forces can be easily obtained. They are not presented herein.

The incremental energy dissipation per length unit along a velocity discontinuity or a narrow transition zone can be expressed as follows:

$$\Delta D_L = c.\Delta V.\cos\phi \qquad (2)$$

where ΔV is the incremental displacement or velocity which makes an angle ϕ with the velocity discontinuity according to the associated flow rule of perfect plasticity, and c is the cohesion parameter. The incremental energy dissipation along the different velocity discontinuities can be easily calculated. They are not presented herein.

Finally, it is to be noted that along the soil-structure interface where we have adopted the assumption of sliding by friction, the energy dissipation is given as follows:

$$\Delta D_L = P.\tan\delta.V_{01} \qquad (3)$$

By equating the total external work to the total internal energy dissipation, we have:

$$P = \frac{1}{2}\gamma.h.H.M_\gamma + c.h.M_c + q.h.M_q \qquad (4)$$

where M_γ, M_c and M_q are the non dimensional anchor force coefficients.

4 NUMERICAL RESULTS

The failure load of anchors can now be obtained by minimisation of P with respect to the angular parameters describing each of the three mechanisms.

Remember here that M_1, M_2 and M_3 are described respectively by one, three and two angular parameters. Three computer programs have been developed with equation (4) as a basis. The programs give the critical slip surface and the corresponding critical failure load P.

In the following sections, we present the M_γ, M_c and M_q values for the three mechanisms as obtained from the numerical extremisation of these coefficients.

4.1 Influence of the embedment depth on the anchor force coefficients

Figure (5) shows the variation of the anchor force coefficients M_γ, M_c and M_q as function of ϕ for two values of the embedment ratio H/h (H/h=1 ; 5) when Ψ=90° and $\delta/\phi = 2/3$. The solutions presented in these figures concern the results obtained from the three mechanisms M_1, M_2 and M_3.

From these figures, one can easily see that the M_1 mechanism highly overestimates the anchor force coefficients especially for the high embedment ratio H/h and for the high ϕ-values. For example, the M_1 mechanism overestimates the M_c value by about 270% compared to the M_2 and M_3 mechanism when Ψ=90°, $H/h = 5$, ϕ = 40° and δ/ϕ=2/3.

The comparison of the solutions given by the M_2 and M_3 mechanisms shows that the results of the M_γ coefficient are approximately identical for both mechanisms. The percent difference does not exceed 5% for Ψ=90°, $H/h = 5$, ϕ = 40° and δ/ϕ=2/3.

However, for the M_c and M_q coefficients, the numerical results (figure 5) show that the M_2 mechanism gives better solutions than the M_3 mechanism since the corresponding upper bound solution is smaller. This remark is only valuable for high values of the embedment ratio H/h. Notice however, that both mechanisms give approximately the same results for small values of the embedment ratio H/h.

4.2 Influence of the anchor inclination on the anchor force coefficients

To show the influence of the anchor inclination on the anchor force coefficients, we first present the results of the anchor plate for Ψ=45°.

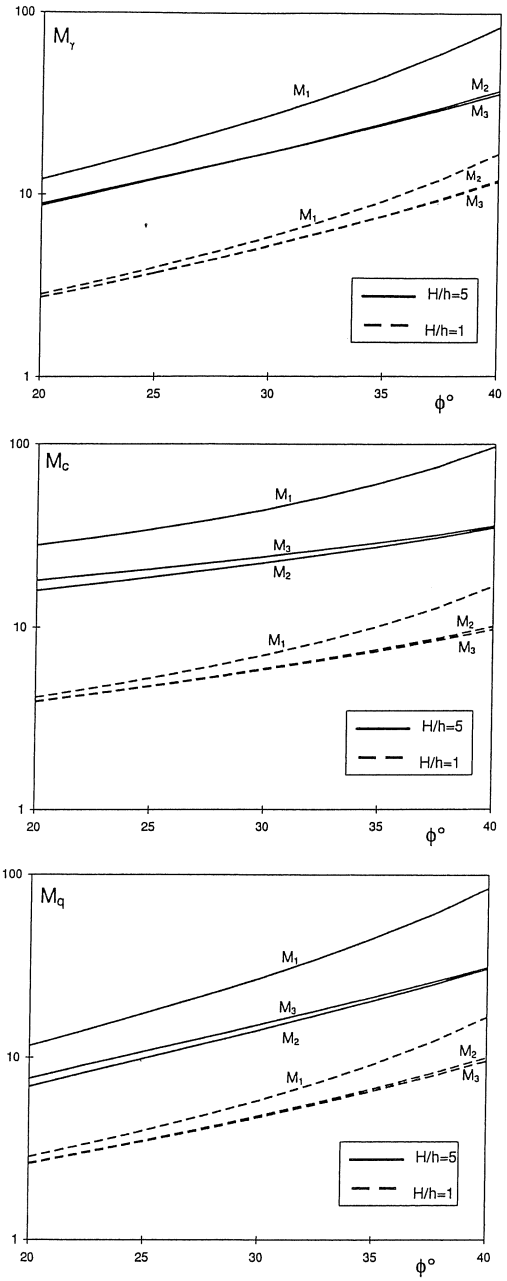

Figure 5 : Anchor force coefficients M_γ, M_c and M_q (Ψ=90°, δ/ϕ=2/3)

Abbildung 5 : Belastungskoeffiziente der Verankerung M_γ, M_c and M_q (Ψ=90°, δ/ϕ=2/3)

Secondly, we present the comparison with the results given above for Ψ=90°.

Figure (6) shows the variation of the anchor force coefficients M_γ, M_c and M_q as function of ϕ for Ψ=45°, H/h=5 and $\delta/\phi = 2/3$. As mentioned in the preceding section, the solutions presented in these figures concern the results obtained from the three mechanisms M_1, M_2 and M_3.

The comparison of the solutions of the M_1 and M_3 mechanisms shows that the results of the M_γ factor are approximately identical for both mechanisms. The difference between the results of both mechanisms slightly increases for the M_c and M_q factors. As in the preceding section, the M_1 mechanism continues to overestimate the anchor force coefficients.

Finally, notice that the numerical results of all coefficients M_γ, M_c and M_q show that the M_2 mechanism gives better solutions than the M_3 mechanism since the corresponding upper bound solution is smaller.

The comparison of the force anchor coefficients for different anchor inclinations show that these coefficients decrease with the anchor inclination decrease. For example, the percent reduction of the M_γ value as given by the M_3 mechanism is about 58% when the anchor inclination varies from 90° to 45° for H/h=5, ϕ=40°, δ/ϕ=2/3.

4.3. Critical slip surfaces

Figure (7) show the critical slip surfaces of the M_1, M_2 and M_3 mechanisms as obtained from the numerical extremisation of the anchor force coefficient M_γ with respect to the angular parameters. These surfaces concern the case of an anchor with the following characteristics: Ψ = 45° & 90°, H/h=2, ϕ=20° & 40° and δ/ϕ=2/3.

As it is well known in the passive earth pressure problem, the M_1 mechanism highly overestimates the failure load due to the fact that the slip surface is far from a planar surface especially for the high values of Ψ, ϕ and δ.

The M_2 and M_3 mechanisms allow the slip surface to develop below the horizontal direction passing through the bottom of the plate anchor. These mechanisms can estimate the anchor force coefficient with good accuracy especially for high values of ϕ, δ and Ψ.

Finally, one can easily see that the slip surfaces tend to planar surfaces when the anchor

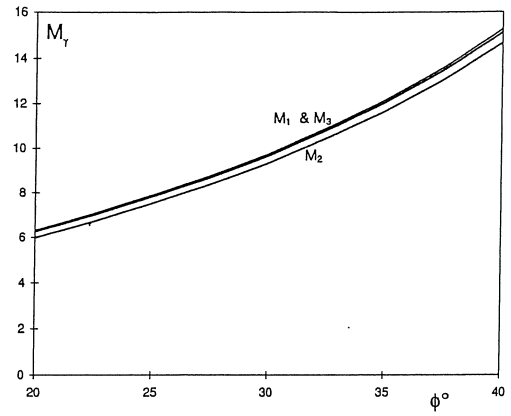

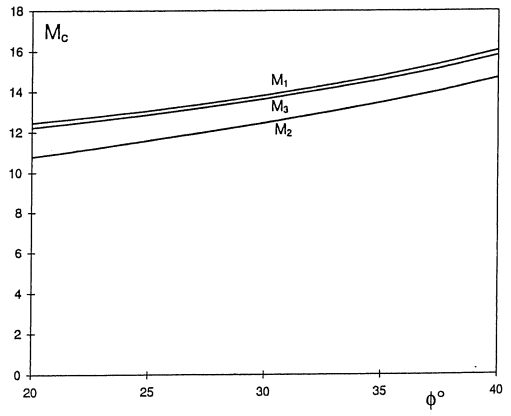

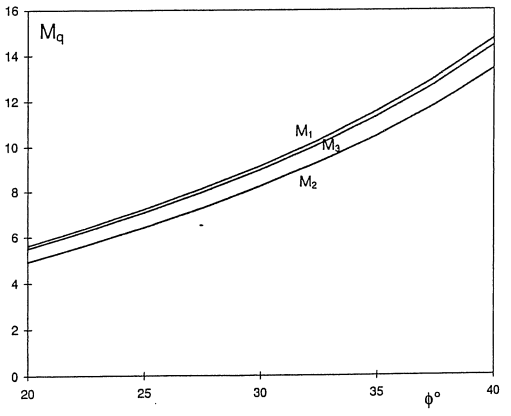

Figure 6 : Anchor force coefficient M_γ, M_c and M_q (Ψ=45°, H/h=5, δ/ϕ=2/3)

Abbildung 6 : Belastungskoeffiziente der Verankerung M_γ, M_c and M_q (Ψ=45°, H/h=5, δ/ϕ=2/3)

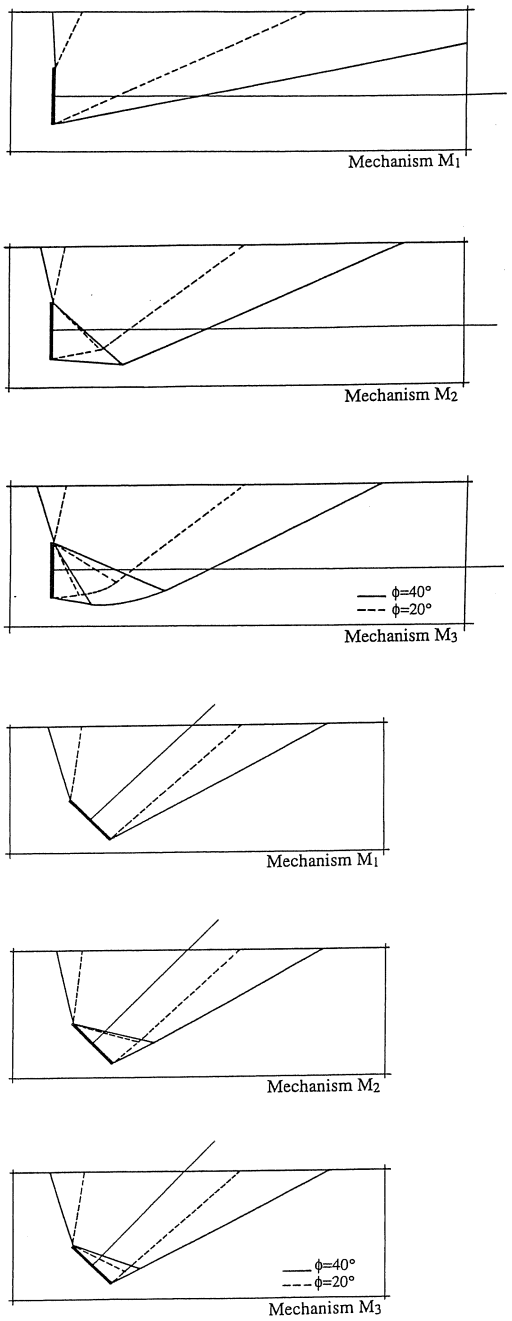

Figure 7 : Critical slip surfaces (H/h=2, Ψ=45° & 90°, ϕ=20° & 40°, δ/ϕ=2/3)

Abbildung 7 : Kritische gleitflachen (H/h=2, Ψ=45° & 90°, ϕ=20° & 40°, δ/ϕ=2/3)

inclination decreases. The radial shear zone of the log sandwich mechanism M_3 disappear. For the two-bloc mechanism M_2, the velocity discontinuity between the two blocs vanishes. Hence, the mechanisms M_2 and M_3 tend to the case of the unique bloc mechanism M_1 for small values of the anchor inclination.

5 CONCLUSION

The upper bound method in limit analysis is used to calculate the anchor force coefficients of a plate anchor. Three failure mechanisms are considered in this analysis. The unique rigid bloc highly overestimates the load anchor for high values of ϕ, δ and Ψ. However, the two-blocs and the log-sandwich mechanisms give results which are in reasonable agreement.

REFERENCES

Chen, W.F. 1975. Limit Analysis and Soil Plasticity. Amsterdam, *Elsevier*, 637p.

Das, B.M. & Seely, G.R. 1975. Pullout Resistance of Vertical Anchors. *J. Geotech. Engng. Div. Am. Soc. Civ. Engrg.*, 101, GT1, 87-91.

Dickin, E.A., & Leung, C.F. 1983. Centrifugal Model Tests on Vertical Anchor Plates, *J. of Geotech. Engng., ASCE*, Vol 109, N° 12, 1503-1525.

Drucker, D.C., Greenberg, H.J. & Prager, W. 1952. Extended limit design theorems for continuous media, *Q. Appl. Math.*, 9, 381-389.

Murray, E.J., & Geddes, J.D. 1989. Resistance of passive inclined anchors in cohesionless medium. *Géotechnique*, Vol 39, N° 3, 417-431.

Neely, W.J., Stewart, J.G., & Graham, J. 1973. Failure Loads of Vertical Anchor Plates in Sand. *J. Soil Mech. Fdns. Div. Am. Soc. Civ. Engng.*, 99 SM9, 669-685.

Ovesen N.K. & Stroman H., 1972. Design methods for vertical anchor plates in sand. *Proceedings of Specialty Conference on Performance of Earth at Earth Supported Structures*, New-York, ASCE, 1481-1500.

Rowe, R.K., & Davis, E.H. 1982. The Behaviour of Anchor Plates in sand. *Géotechnique*, Vol 32, N° 1, 25-41.

Smith, J.E., 1962. Deadman anchorages in sand. *Technical report R199. US Naval Civil Engineering Laboratory*, Port Hueneme.

Smith, J.E., 1966. Deadman anchorages in various soil mediums. *Technical report R434. US Naval Civil Engineering Laboratory*, Port Hueneme.